



Fabrication and characterization of stir casting AA6061–31%B₄C composite

Yu LI^{1,2}, Qiu-lin LI¹, Dong LI^{1,2}, Wei LIU², Guo-gang SHU³

1. Graduate School at Shenzhen, Tsinghua University, Shenzhen 518055, China;
2. School of Materials Science and Engineering, Tsinghua University, Beijing 100084, China;
3. Nuclear Materials Joint Laboratory, Tsinghua University, Shenzhen 518055, China

Received 6 September 2015; accepted 6 January 2016

Abstract: A sophisticated stir casting route to fabricate large scale AA6061–31%B₄C composite was developed. Key process parameters were studied, microstructure and mechanical properties of the composite were investigated. The results indicated that vacuum stirring/casting, B₄C/Mg feeding and ingots cooling were essential to the successful fabrication of AA6061–31%B₄C composite. Chemical erosion examination verified the designed B₄C content; X-ray fluorescence spectrometer (XFS) showed the chemical composition of Mg and Si in the matrix conformed to industry standards; scanning electronic microscope (SEM) and X-ray diffraction (XRD) revealed that B₄C particles were evenly distributed in the composites with well dispersed Mg₂Si precipitates. Tensile testing results showed that the AA6061–31%B₄C composite had a tensile strength of 340 MPa, improved by 112.5% compared with AA1100–31%B₄C composite, which is attributed to the enhanced strength of the matrix alloy.

Key words: Al–B₄C alloy; metal matrix composite; stir casting; microstructure; mechanical properties

1 Introduction

Al–B₄C metal matrix composites (MMCs) combine the desirable attributes of aluminum and boron carbide. Al matrix has low density, resists corrosion and provides a wide range of strength levels by adding various alloy elements with their subsequent aging hardening [1]. As the reinforcing phase, B₄C is a hard material (surpassed only by diamond and cubic boron nitride) with excellent thermal stability, high wear resistance and large neutron absorption cross section [2,3]. Therefore, Al–B₄C composites are widely used in automotive, aerospace, military industry, especially in nuclear industry for storage and transportation of spent fuels [4–7], and the application is expected to increase with the development of low-cost processing methods.

Among the available manufacturing processes, stir casting is appealing for its flexibility in selecting raw materials and processing conditions, through which composites with various matrixes and reinforcing phases have been successfully fabricated [8–12]. It is also attractive for being economical, allowing large scale composites to be fabricated [13]. However, major challenges lie in wetting and chemical reactions between

the ceramic particles and the matrix, homogeneous distribution of reinforcement materials, fluidity of the composites and porosity in the cast metal matrix composites [14], and wide adoption of stir casting method depends on a satisfactory resolution of these technical difficulties.

In fabricating Al–B₄C stir casting composites, Ti was found to be an effective alloy element for promoting the wetting between B₄C and molten aluminum, as well as limiting the degradation of B₄C particles [15,16]. Ti-rich layer was formed around B₄C particle surfaces and this layer was identified to be TiB₂ at a reaction temperature of 750 °C [17]. Based on this, extensive researches have been conducted on Al–B₄C [18], Al–Si–B₄C [19], Al–Mg–B₄C [20], Al–Mg–Si–B₄C [9,10] composites concerning interface, particle distribution, fluidity and mechanical strength of the composites. However, B₄C content in these composites was low, typically with mass fractions less than 15%. For both functional and structural purposes, it is desirable to fabricate Al–B₄C composite with high B₄C content and high strength matrix [6,21–23]. In this work, AA6061–31%B₄C composite was fabricated. On the one hand, it is an endeavor to develop competitive stir casting Al/B₄C composites where their powder metallurgy counterparts

have been prevalent in nuclear industry for storage and transportation of spent fuels [4,21]; on the other hand, the successful processing of composites with high B_4C content and high strength matrix would indicate sophisticated handle of stir casting method which would further expand its applications. As anticipated, difficulties associated are exacerbated. Major challenges involve incorporation and dispersion of lots of B_4C particles, fluidity deterioration during stirring and casting, and chemical composition control of the matrix.

Based on these considerations, a sophisticated stir casting technique was developed to fabricate large scale (about 12 kg per batch) AA6061–31% B_4C (mass fraction) composite. Key process parameters were studied, the microstructure and mechanical properties of the composite were investigated.

2 Experimental

2.1 Composites preparation and rolling

Figure 1 shows the schematic of the designed equipment used in the experiment. A graphite crucible was placed at the center of the furnace with induction heating coil around. Two thermocouples were set outside and inside of the crucible respectively for heating control. At the bottom of crucible there was a hole with tightly matched stopper, which was designed to pour the composite slurry into the mold consecutively at the end of the mechanical stirring. The mechanical stirrer system was along the axis of the crucible which was able to rotate and adjust its height consecutively. The feeding tank was designed to add ceramic powders and alloy

elements at proper time during the stir casting. The vacuum valve provided the whole system with a vacuum limit about 10 Pa, while argon gas was used to balance the atmosphere pressure in cases that the mold separated from the furnace to cool in air. The shape and size of the impeller blade are also shown in Fig. 1. It is a simplified version of a typical three-blade propeller. It has two blades to gain better strength considering the paramount resistance encountered during stir casting. The edge-lengths of the cut parts (two parts are symmetric) are 60, 30 and 30 mm, respectively.

Initially, calculated commercial pure Al (99.7%), Al–20%Si master alloy, Al–10%Ti (mass fraction) master alloy were melted in the graphite crucible and maintained at 750 °C, and B_4C powders were preheated at 400 °C for 2 h. Then, the furnace was open to remove the slag of the melt. Meanwhile, calculated commercial pure Mg (99.99%) and preheated B_4C particles with an average size of 23 μm were placed in the feeding tank. After the system approached its vacuum limits, B_4C powders were added into the melt approximately at the speed of 1000 g/min. The melt was stirred after incorporation of particles in the melt at gradually increasing speed and hold at 550 r/min after all the B_4C powders were added. The stable vortex lasted for 15 min, and Mg granules were added into the melt in the final 1 min. Finally, the stirrer was turned off, the stopper was pulled down, and the composite slurry was poured in a preheated rectangular heat-resistant steel mold (450 °C) which was then separated from the furnace for cooling. Table 1 lists key processes studied. With optimized process, two experimental composites namely

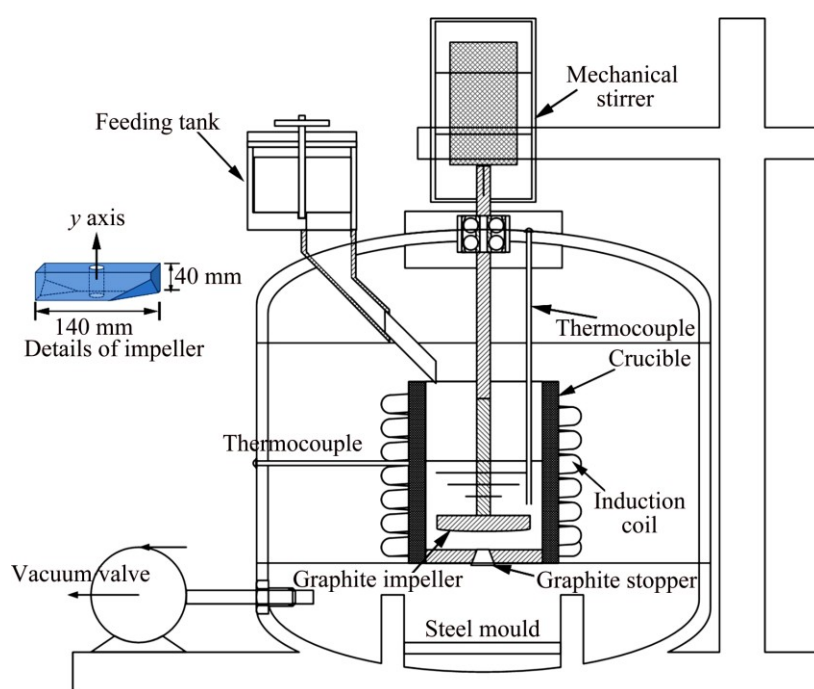


Fig. 1 Schematic of designed equipment

Table 1 Key processes and composites fabricated in experiment

Process	Composite fabricated
Vacuum/stirring	AA1100–15%B ₄ C
Vacuum/casting	AA1100–31%B ₄ C
B ₄ C/Mg feeding	AA6061–31%B ₄ C
Ingot cooling	

AA1100–31%B₄C and AA6061–31%B₄C containing 3.5% Ti (mass fraction) were prepared for comparison.

Hot rolling of the composites was carried out at 400 °C to avoid Al matrix hardening. For every rolling pass, rolling reduction was fixed at 1 mm and rolled sheet was reheated at 400 °C for 15 min. Finally, ingots were rolled into 3 mm sheets to evaluate their microstructure and mechanical properties.

2.2 Heat treatment

Samples for mechanical properties evaluation were subjected to modified T6 heat treatment. Solution temperature was elevated to 570 °C considering that at higher solution temperature, the greater degree of supersaturation will cause more Mg₂Si precipitates to form in the matrix-rich zones of the composites [24].

Samples for chemical composition evaluation were held at 570 °C for 30 min and then quenched in water to ensure homogeneous distribution of alloy elements in the matrix.

2.3 Characterization

B₄C content was determined with chemical method. Five samples representative with dimensions of 50 mm × 25 mm × 3 mm were first fully eroded in NaOH solution (1 mol/L) for 24 h, respectively. After carefully filtering the clean liquid, appropriate content HCl solution was added to balance surfeit NaOH solvent. The solution was stirred vigorously before another 24 h of standing. Finally, B₄C powders were filtered and dried for weighing.

The chemical composition of matrix was determined by X-ray fluorescence spectrometer (XFS, ARL Perform'X 4200). X-ray diffraction (XRD) measurements were conducted with a Rigaku D/max 2500 VB2+/PC, operated at 40 kV and 100 mA to produce Cu K_α radiation ($\lambda=1.54 \text{ \AA}$). A scanning electronic microscope (SEM, TESCAN MIRA 3 LMH), equipped with an energy dispersive spectrometer (EDS) was used to examine the particle distribution and interfaces of the composites. Samples for Al/B₄C interface observations were prepared by mechanical and ion beam (IB-09020CP, JEOL) polishing methods, successively.

Tensile test samples were machined into rectangular specimens, conforming to ASTM E8M standards for

subsize specimens, with a gauge length of 25 mm. The mechanical response was measured on a MTS servohydraulic universal testing machine with a strain rate of $1 \times 10^{-3} \text{ s}^{-1}$, and each average value was obtained from four tensile tests.

3 Results and discussion

3.1 Key process parameters

3.1.1 Vacuum stirring/casting

In the stir casting technique, vortex is the major drive force to create and maintain a good distribution of the reinforcement material in the matrix alloy. However, a vigorously stirred melt will entrap air bubbles which are proved to be extremely difficult to be removed as the viscosity of the slurry increases. The entrapped gas weakens the wettability between B₄C particles and molten aluminum by forming gas layer surrounding particles and results in high porosity and inclusions in the cast product [14].

Vacuum stir casting is effective to eliminate the entrapment of external gas onto melt and oxidation of aluminum during stirring synthesis [25]. Figure 2 shows the microstructures of AA1100–15%B₄C composites fabricated under atmospheric pressure and 10 Pa, respectively. Dark region around B₄C particles indicates porosity or clusters in the microstructure. In comparison,

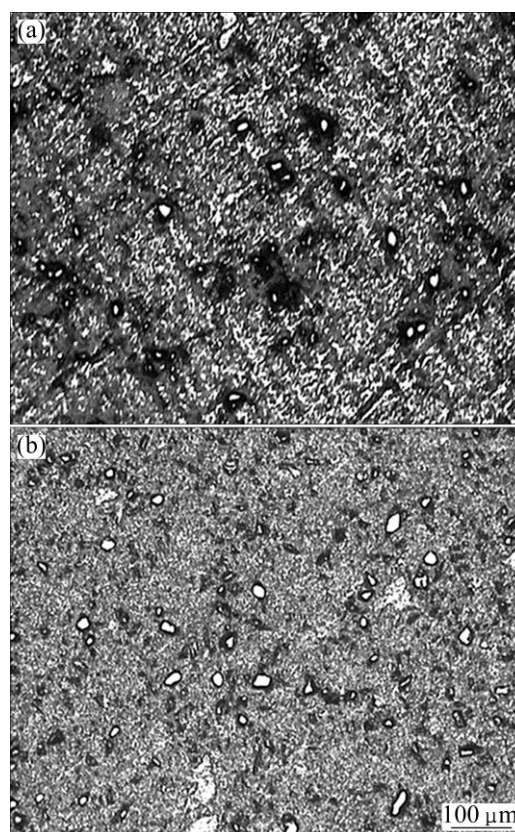


Fig. 2 Microstructures of AA1100–15%B₄C composite fabricated under atmospheric pressure (a) and 10 Pa (b)

composites fabricated under vacuum stirring show more uniform particle distribution and neat microstructure. In addition, due to detrimental effect of entrapped gas, AA6061–31%B₄C composite was unable to be fabricated under atmospheric pressure. Typically, the B₄C particles floated on the surface, indicating poor wettability between B₄C particles and Al matrix. Therefore, to fabricate AA6061–31%B₄C composites, vacuum stirring is essential considering the amount of B₄C particles which need to be incorporated and dispersed.

Vacuum condition also matters in the casting period since fluidity is crucial for mold filling. For composite with B₄C content as high as 31% (mass fraction), fluidity deteriorated rapidly when the crucible was exposed in air due to temperature drops and contact with air. Figure 3 shows composites cast in air. Even the mold was preheated and vibrated during casting to promote fluidity of the composite slurry, surface defects like wrinkles and bulges were apparent, which indicated limited fluidity during mold filling. In comparison, composites cast consecutively with the designed stopper showed neat surface resulting from excellent fluidity (Fig. 4(b)).



Fig. 3 Typical surface defects of composites cast in air

3.1.2 B₄C/Mg feeding

The feeding tank was designed to add large quantity of B₄C particles. By adding B₄C particles progressively, the stirrer got the particles dispersed in the melt step by step to ensure homogeneous distribution. Since the melt was alloyed with Ti, the added B₄C particles were stable in the melt and were not different from subsequently added B₄C particles in morphology. In practice, another method was tried. B₄C particles were packed together with aluminum foil and added into the melt all at once. Results showed that graphite impeller broke frequently at the initial stage of stirring and B₄C powder ring formed on the crucible wall during the stirring due to massive B₄C powders.

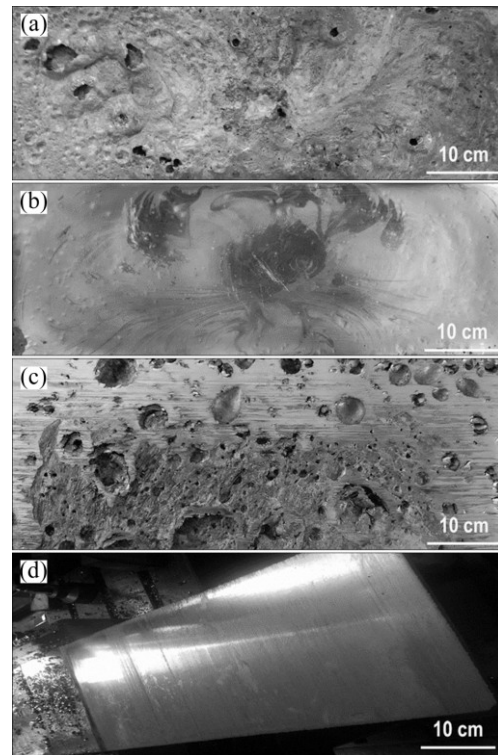


Fig. 4 Ingot surface morphologies of AA6061–31%B₄C composites cooled under different conditions: (a) In furnace; (b) In air; (c) In furnace, 5 mm under surface; (d) In air, 5 mm under surface

Unlike the report in other articles, desired aluminum alloys were directly melted at the first stage [9,10], which causes chemical composition deviation of the matrix material. In our experiments, calculated Al–20%Si master alloy was firstly melt with the pure aluminum, and then pure Mg was added into the melt in the final 1 min of the stirring. Reasons behind are two, on one hand, Mg is highly volatile and easily loses during the stir casting, this adjustment prevents Mg from long time exposure to high temperature; on the other hand, before Mg was added, TiB₂ layer had already formed on B₄C particle surfaces. Therefore, detrimental effect of Mg on Al–B₄C interfacial reactions was inhibited [19].

Table 2 shows Mg and Si contents of AA6061–31%B₄C composites fabricated through two methods. Considering that Si is stable, the mass ratio of Mg/Si should be an effective indicator showing the variation of Mg content during different procedures. In the conventional procedure, the ratio is 0.591, while the raw material has a ratio of 2 as shown in the parentheses. In the modified procedure, the ratio is 1.434 compared with the designed ratio of 1.25. This proves that the modified procedure inhibited Mg loss during the stir casting which is responsible for fabricating Al–B₄C

composites with precise matrix chemical composition. Also, the Mg and Si contents in the matrix confirm to AA6061 industry standards. More importantly, this procedure enables us to adjust Mg and Si contents flexibly and consequently provides wide range of strength levels.

Table 2 Mg and Si contents of composites fabricated under different procedures

Procedure	w(Mg)/%	w(Si)/%	Mass ratio of Mg to Si
Conventional	0.467	0.79	0.591 (2)
Modified	0.826	0.576	1.434 (1.25)

3.1.3 Ingots cooling

Since Mg is highly volatile, different cooling conditions result in distinctive ingot surface morphologies. Figure 4(a) shows ingot surface morphology cooling in furnace. Bulges and dimples are scattered around the surface. Figure 4(c) reveals fresh surface 5 mm under position where concaves are more apparent. At the initial stage of the solidification, temperature was still high, magnesium steam formed bubbles in the matrix and floated near the surface. Because the melt was viscous and the surface solidified quickly, the bubbles were trapped in the matrix near the surface and formed the final surface morphology. In comparison, ingot cooling in air shows neat surface and compact microstructure.

3.2 Characterization

3.2.1 Chemical composition

The contents of B₄C determined with chemical method are shown in Fig. 5. By taking samples from representative positions illustrated in Fig. 5, the results are informative in two aspects. On one hand, B₄C content fluctuating around 31% reveals that the designed B₄C content was incorporated within acceptable error range; on the other hand, it shows that the B₄C particles were evenly distributed on a relatively macro level.

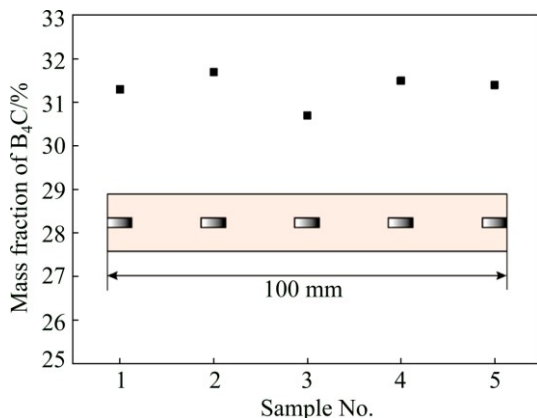


Fig. 5 B₄C contents of different samples from representative positions

Table 2 shows Mg and Si contents of AA6061–31%B₄C composites fabricated by starting with AA6061 aluminum alloy and by adding Mg and Si respectively. As analyzed previously in Section 3.1.2, it proves that the modified procedure inhibits Mg loss during the stir casting which is responsible for fabricating Al/B₄C composites with precise chemical composition.

3.2.2 Microstructure analysis

Figure 6 shows particle distribution of AA6061–31%B₄C composites in as-cast and as-rolled conditions, respectively. Previous study on Al–7%Si–10%B₄C die casting composite [26] characterized solidification and fluid flow processes as two major factors contributed to particle distribution. On one hand, particles were pushed by the growing primary α (Al) grains. Particle network was highlighted in Fig. 6(a) where light particle inside was Al₃Ti which came from excessive Al–Ti master alloy. Since Al₃Ti intermetallic particles were effective nucleants during solidification [27], they were at the core of growing α (Al) grains and with B₄C particles pushed away. On the other hand, the particles in the dispersion

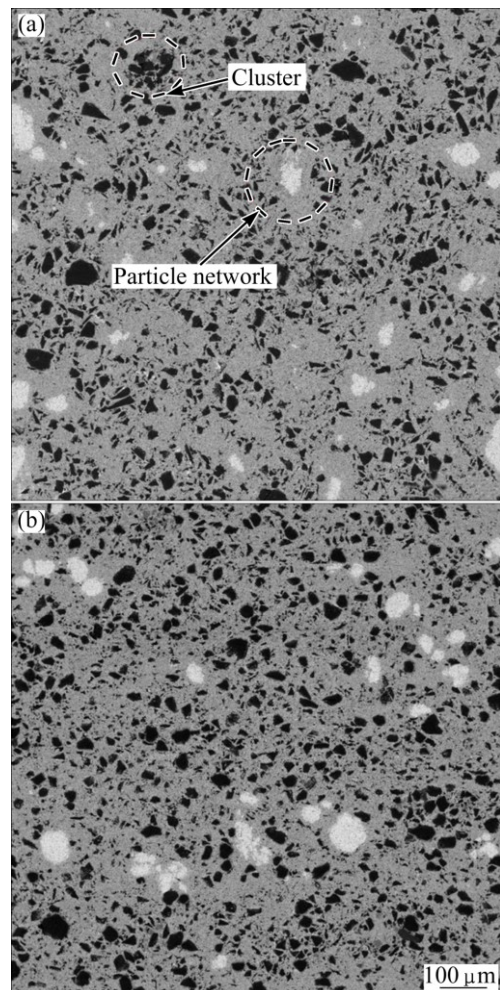


Fig. 6 Particle distribution of AA6061–31%B₄C composites: (a) As-cast; (b) As-rolled

system moved towards the center where shearing is at a minimum [28]. However, a segregation band where the amount of B_4C particles is less in the regions near the mold walls than that in the center was not observed due to high preheating temperature of the mold [26]. Cluster of B_4C was also highlighted in Fig. 6(a) which is evitable during stir casting. As a consequence, rolling process

was employed to get uniform particle distribution. Figure 6(b) shows particle distribution of composites after rolling. Cluster and particle network were significantly reduced, which is beneficial to the mechanical properties of the composites.

Figure 7(a) shows high magnification SEM backscattered electron image of the composite. Light

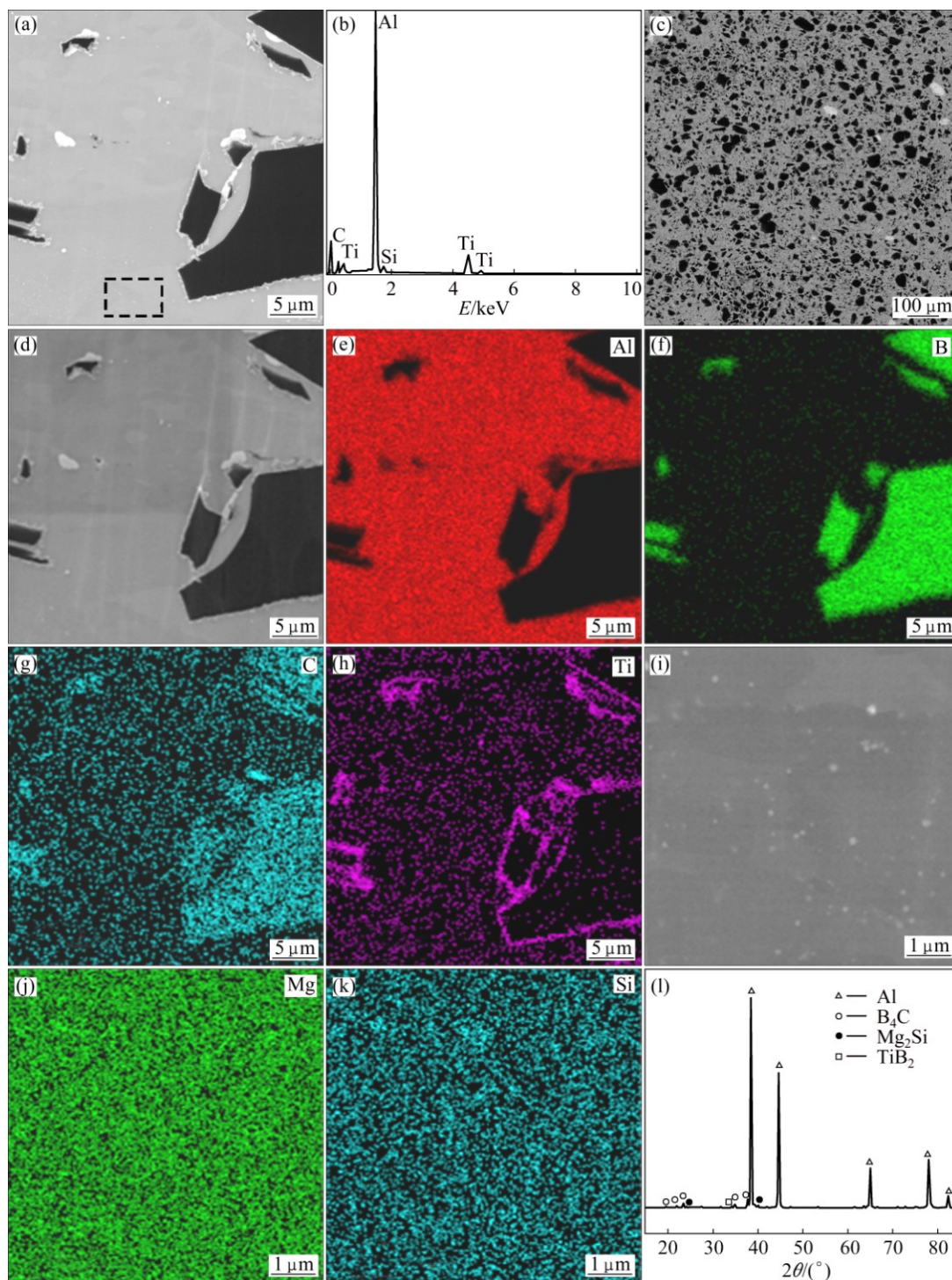


Fig. 7 Microstructures of AA 6061–31% B_4C composite: (a) High magnification SEM backscattered electron image; (b) EDS pattern; (c) Low magnification SEM backscattered electron image; (d) Low magnification electron image; (e–h) Al, B, C and Ti elemental mappings, respectively; (i) SEM image of local zone in (a); (j, k) Mg and Si elemental mappings, respectively; (l) XRD pattern showing the presence of TiB_2 and Mg_2Si in composite

particles were found to be Al_3Ti with traceable C and Si elements. It corresponds to the bright zone in Fig. 7(c), which came from the Al–Ti master alloy. Figure 7(c) shows low magnification SEM backscattered electron image of AA6061–31% B_4C composite. Dark B_4C particles are evenly distributed in the matrix. Figures 7(d) and (e–h) show elements distribution of Al, B, C and Ti. The results are according with former research as Ti-rich layer formed around B_4C particle surfaces. This Ti-rich layer was identified as TiB_2 in previous studies [17] since under the experimental temperature, the following reaction happened:



The formation of TiB_2 layer has been shown to limit the decomposition of B_4C particles and promote their wettability in liquid aluminum which is a breakthrough facilitating the fabrication of Al– B_4C composites with stir casting technique. Also, the bonding between Al and B_4C is quite stable during deformation.

Figure 7(i) shows SEM image of local zone in Fig. 7(a) which shows presence of fine light particles. Figures 7(j) and (k) are elemental mapping results. Mg and Si elements show no segregation accordingly because the particles are too small compared with the spot size of energy dispersive spectrometer (EDS). X-ray diffraction (XRD) pattern in Fig. 7(l) shows the presence of Mg_2Si . Combining the X-ray fluorescence spectrometer (XFS), SEM and X-ray diffraction (XRD) results, it is safe to conclude that those fine light particles are Mg_2Si . Also, it should be noted that the X-ray is insensitive to B_4C as reported in other studies [29], therefore, despite the high B_4C content, its corresponding peak is weak.

3.2.3 Tensile strength

As shown in Fig. 8, the ultimate tensile strength (UTS) of Al– B_4C composite improved significantly after alloying Mg and Si elements. The average UTS of AA6061–31% B_4C composite is 340 MPa, improved by 112.5% comparing with 160 MPa of AA1100–31% B_4C composite. The elevation in tensile strength could be easily interpreted in terms of rule of mixtures. The tensile strengths of commercial pure aluminum AA1100 (O) and aluminum alloy AA6061 (T6) are approximately 80 and 280 MPa [30], respectively. Then, it can be calculated that the B_4C reinforcement contributed 80 MPa to the total tensile strength. So, the elevation in tensile strength after alloying Mg and Si elements is attributed to the intrinsic strength of the matrix alloy which is in accordance with previous study on SiC particulate-reinforced Al–Zn–Mg–Cu composites where SiC has similar size of approximately 30 μm [31]. It should be noted that 31% B_4C only contributed about 80 MPa while 1% Mg and 0.8% Si together contributed about 180 MPa to the total strength. Since B_4C particles

are at micrometric level, the strengthening mechanisms are load transfer and interaction between dislocations and “dislocation punched zones” formed in the vicinity of reinforcement/matrix interface [27]. For AA6061 aluminum alloy, precipitated nanoscale Mg_2Si phase due to T6 heat treatment provides the enhanced strength in a more effective way of Orowan mechanism [32].

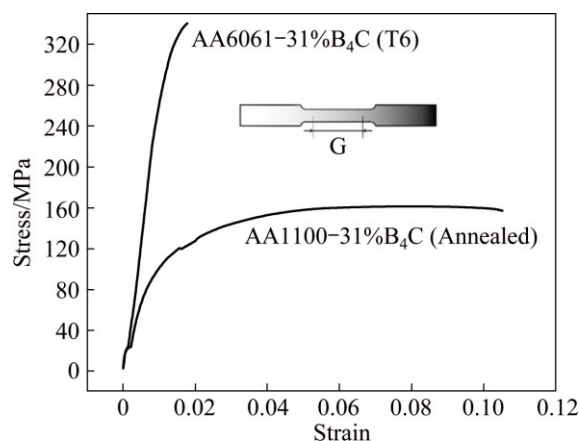


Fig. 8 Stress–strain curves of AA6061–31% B_4C and AA1100–31% B_4C composites

Tensile strength was increased at the expense of plasticity. The average elongation values of AA1100–31% B_4C and AA6061–31% B_4C composites are 7.52% and 1.61%, respectively. Figure 9 shows tensile fracture surfaces of the two composites. B_4C particles in both composites act as void initiation sites. In Fig. 9(a), dimples are larger and deeper, indicating better plasticity, because the matrix is pure aluminum. In contrast, dimples around B_4C particles in Fig. 9(b) are less obvious since the matrix is AA6061 aluminum alloy which has less plasticity. Also, fine dimples in the matrix are corresponding to fine Mg_2Si precipitates. It should also be noted that cracked B_4C particles and their intact Al/ B_4C interfaces manifest that the reinforcement/matrix interface is stable enough under applied load.

4 Conclusions

1) Al– B_4C composites were fabricated by modified stir casting technique with high B_4C content (up to 31%, mass fraction) and precise chemical composition (AA6061). Key process parameters were studied, microstructure and mechanical properties of the composites were investigated.

2) Vacuum stirring and adding B_4C powder progressively are essential to incorporate high content B_4C ; adding Mg and Si respectively are necessary to get precise matrix chemical composition; vacuum casting and cooling ingots in air are responsible for excellent mold filling and Mg maintenance.

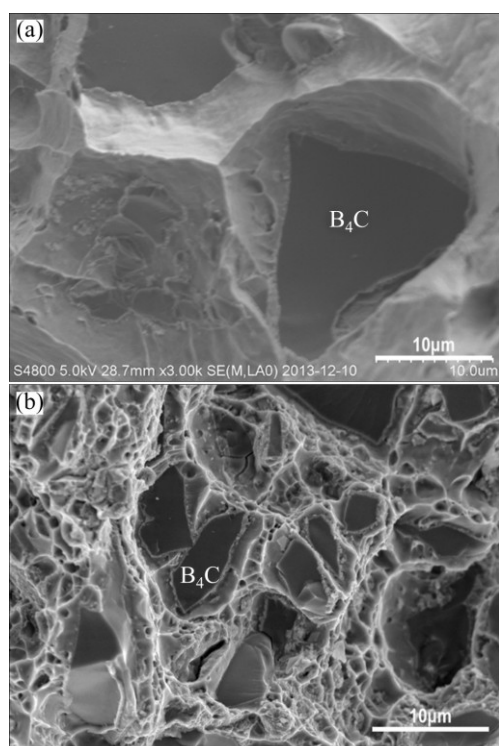


Fig. 9 Tensile fracture surfaces of AA1100–31%B₄C (a) and AA6061–31%B₄C (b) composites

3) Chemical erosion examination showed that the designed B₄C content was incorporated; X-ray fluorescence spectrometer (XFS) showed that the chemical composition of the matrix conformed to AA6061 industry standards; scanning electronic microscope (SEM) and X-ray diffraction (XRD) revealed that B₄C particles were evenly distributed in the matrix with well dispersed fine Mg₂Si precipitates.

4) AA6061–31%B₄C composite had a UTS of 340 MPa, improved by 112.5% compared with AA1100–31%B₄C composite, which is attributed to the significantly enhanced strength of the matrix after alloying Mg and Si elements. It covers a board range of B₄C content and mechanical strength levels, making it the best candidate for Al–B₄C composites applications. Furthermore, the illustrated stir casting technique is promising in increasing the number of applications of Al–B₄C composites.

Acknowledgments

This work was funded by Joint Laboratory of Nuclear Materials and Service Safety (2013966003), China and the authors thank Dr. Liang WANG for useful discussion. The authors also thank Mr. Ji-yun ZHENG at Tsinghua University for experimental assistance.

References

[1] POLMEAR I J. Aluminum alloys—A century of age hardening [J].

Materials Forum, 2004, 28: 1–14.

- [2] THEVENOT F. Boron carbide—A comprehensive review [J]. Journal of the European Ceramic Society, 1990, 6: 205–225.
- [3] DOMNICH V, REYNAUD S, HABER R A, CHHOWALLA M. Boron carbide: structure, properties, and stability under stress [J]. Journal of the European American Society, 2011, 94: 3605–3628.
- [4] MACHIELS A, LAMBERT R. Handbook of neutron absorber materials for spent nuclear fuel transportation and storage applications [M]. Palo Alto: EPRI, 2009.
- [5] PRASAD S V, ASTHANA R. Aluminum metal–matrix composites for automotive applications: Tribological considerations [J]. Tribology Letters, 2004, 17: 445–453.
- [6] CHEN X G, HARK R. Development of Al–30% B₄C metal matrix composites for neutron absorber material [C]//Aluminum alloys: Fabrication, Characterization and Applications. New Orleans: TMS, 2008: 3–9.
- [7] KALAISELVAN K, MURUGAN N. Role of friction stir welding parameters on tensile strength of AA6061–B₄C composite joints [J]. Transactions of Nonferrous Metals Society of China, 2013, 23: 616–624.
- [8] SHOROWORDI K M, LAOUI T, HASEEB A S M A, CELIS J P, FROYEN L. Microstructure and interface characteristics of B₄C, SiC and Al₂O₃ reinforced Al matrix composites: A comparative study [J]. Journal of Materials Processing Technology, 2003, 142: 738–743.
- [9] KALAISELVAN K, MURUGAN N, PARAMESWARAN S. Production and characterization of AA6061–B₄C stir cast composite [J]. Materials and Design, 2011, 32: 4004–4009.
- [10] TOPTAN F, KILICARSLAN A, KARAASLAN A, CIGDEM M, KERTI I. Processing and microstructural characterization of AA1070 and AA6063 matrix B₄C_p reinforced composites [J]. Materials and Design, 2010, 31(S): s87–s91.
- [11] KHOSRAVI H, AKHLAGHI F. Comparison of microstructure and wear resistance of A356–SiC_p composites processed via compocasting and vibrating cooling slope [J]. Transactions of Nonferrous Metals Society of China, 2015, 25: 2490–2498.
- [12] EZATPOUR H R, TORABI-PARIZI M, SAJJADI S A. Microstructure and mechanical properties of extruded Al/Al₂O₃ composites fabricated by stir-casting process [J]. Transactions of Nonferrous Metals Society of China, 2013, 23: 1262–1268.
- [13] SURAPPA M K. Microstructure evolution during solidification of DRMMCs (discontinuously reinforced metal matrix composites): State of art [J]. Journal of Materials Processing Technology, 1997, 63: 325–333.
- [14] HASHIM J, LOONEY L, HASHIM M S J. Metal matrix composites: Production by the stir casting method [J]. Journal of Materials Processing Technology, 1999, 92: 1–7.
- [15] KENNEDY A R. The reactive wetting and incorporation of B₄C particles into molten aluminium [J]. Scripta Materialia, 2001, 44: 1077–1082.
- [16] KENNEDY A R. The microstructure and mechanical properties of Al–Si–B₄C metal matrix composites [J]. Journal of Materials Science, 2002, 37: 317–323.
- [17] ZHANG Z, FORTIN K, CHARETTE A, CHEN X G. Effect of titanium on microstructure and fluidity of Al–B₄C composites [J]. Journal of Materials Science, 2011, 46: 3176–3185.
- [18] ZHANG Z, CHENX G, CHARETTE A. Fluidity and microstructure of an Al–10% B₄C composite [J]. Journal of Materials Science, 2009, 44: 492–501.
- [19] ZHANG Z, FORTIN K, CHARETTE A, CHEN X. Fluidity and microstructure evolution of Al–12%B₄C composites containing magnesium [J]. Materials Transactions, 2011, 52: 928–933.
- [20] HU H M, LAVERNIA E J, HARRIGAN W C, KAJUCH J, NUTT S R. Microstructural investigation on B₄C/Al–7093 composite [J]. Materials Science and Engineering A, 2001, 297: 94–104.

- [21] MACHIELS A. Qualification of METAMIC® for spent-fuel storage application [M]. Palo Alto: EPRI, 2001.
- [22] ZHENG R, CHEN J, ZHANG Y, AMEYAMA K, MA C. Fabrication and characterization of hybrid structured Al alloy matrix composites reinforced by high volume fraction of B₄C particles [J]. Materials Science and Engineering A, 2014, 601: 20–28.
- [23] CHEN H S, WANG W X, LI Y L, ZHANG P, NIE H H, WU Q C. The design, microstructure and tensile properties of B₄C particulate reinforced 6061 Al neutron absorber composites [J]. Journal of Alloys and Compounds, 2015, 632: 23–29.
- [24] AIDUN D, MARTIN P, SUN J. Effects of heat treatment on the mechanical properties of SiC_p/6061 Al composite [J]. Journal of Materials Engineering and Performance, 1992, 1: 615–624.
- [25] GUI Man-chang, HAN Jian-min, LI Pei-yong. Fabrication and characterization of cast magnesium matrix composites by vacuum stir casting process [J]. Journal of Materials Engineering and Performance, 2003, 12: 128–134.
- [26] ZHANG Z, CHEN X G, CHARETTE A. Particle distribution and interfacial reactions of Al–7%Si–10%B₄C die casting composite [J]. Journal of Materials Science, 2007, 42: 7354–7362.
- [27] MOHANTY P S, GRUZLESKI J E. Mechanism of grain refinement in aluminum [J]. Acta Materialia, 1995, 43: 2001–2012.
- [28] FERGUSON J, KEMBLOWSKI Z. Applied fluid rheology [M]. London: Elsevier, 1991.
- [29] ZHANG J, LEE J, CHO Y, KIM S, YU H. Effect of the Ti/B₄C mole ratio on the reaction products and reaction mechanism in an Al–Ti–B₄C powder mixture [J]. Materials Chemistry and Physics, 2014, 147: 925–933.
- [30] ZHENG Feng. Handbook of aluminum and aluminum alloys [M]. Beijing: Chemical Industry Press, 2008. (in Chinese)
- [31] SONG J Y, GUO Q, OUYANG Q B, SU Y S, ZHANG J, LAVERNIA E J, SCHOENUNG J M, ZHANG D. Influence of interfaces on mechanical behavior of SiC particulate-reinforced Al–Zn–Mg–Cu composites [J]. Materials Science and Engineering A, 2015, 644: 79–84.
- [32] KNIPLING K E, DUNAND D C, SEIDMAN D N. Criteria for developing castable, creep-resistant aluminum-based alloys — A review [J]. Z Metallkd, 2006, 3: 246–265.

AA6061–31%B₄C 复合材料的制备与表征

李宇^{1,2}, 李丘林¹, 李栋^{1,2}, 刘伟², 束国刚³

1. 清华大学 深圳研究生院, 深圳 518055;
2. 清华大学 材料科学与工程学院, 北京 100084;
3. 清华大学 核材料联合实验室, 深圳 518055

摘要: 开发一种高效液态搅拌铸造工艺制备 AA6061–31%B₄C 复合材料。研究该工艺的关键参数, 并对复合材料的显微组织和力学性能进行表征。结果表明, 真空搅拌/浇铸、B₄C/Mg 加料方式和铸锭冷却是 AA6061–31%B₄C 复合材料成功制备的关键参数。化学腐蚀检测结果证实复合材料中含有设计含量的 B₄C; X 射线荧光检测表明, 复合材料基体中 Mg 和 Si 含量符合工业标准; 扫描电镜和 X 射线衍射结果表明, B₄C 颗粒均匀分布在基体中, 颗粒之间为时效析出的 Mg₂Si 相; 拉伸结果表明, AA6061–31%B₄C 复合材料的抗拉强度为 340 MPa, 比 AA1100–31%B₄C 复合材料的抗拉强度提高了 112.5%, 这归因于基体铝合金强度的大幅提高。

关键词: Al–B₄C 合金; 金属基复合材料; 搅拌铸造; 显微组织; 力学性能

(Edited by Wei-ping CHEN)